

An XeCl* Excimer Fluorescence Study on the Pulse Radiolysis of Xe–CCl₄ and Xe–SOCl₂ Systems

A. Jówko,^{1,2} J. Kowalczyk,¹ and K. Wojciechowski¹

Received September 28, 1999; revised February 25, 2000; accepted February 28, 2000

The mechanism and kinetics of energy transfer from highly excited Xe states ($E_{\text{ex}} > 9.5$ eV), generated by a 12-ns electron beam, to chlorine donor molecules were deduced from time-resolved spectra of fluorescence in the region 240–340 nm. The emissions at 240–250 nm were assigned to Xe $\ddot{\text{X}}^*$ excimers, and those at 308 and 340 nm to XeCl(B) and XeCl(C) states. Kinetic analysis of the recorded spectra for Xe–CCl₄ and Xe–SOCl₂ gas mixtures at constant xenon pressure and various pressures of molecular admixtures (0.1–1 Torr) allowed us to find the rate constants for the reactions (5) Xe $\ddot{\text{X}}^*$ + RCl → products, (6a) Xe $\ddot{\text{X}}^*$ + RCl → XeCl(B) + R*, and (6b) Xe $\ddot{\text{X}}^*$ + RCl → XeCl(C) + R*, where R is any radical.

KEY WORDS: Gas kinetics; excimers; pulse radiolysis; energy transfer.

INTRODUCTION

Electronic energy transfer processes from the rare-gas excited states to different molecules have been studied in a number of laboratories, mainly for the lowest Xe(6s) and higher Xe(6p) states [1–14]. The interest is due to the importance of these processes in the formation of RgX excimers (Rg = rare gas; X = Cl, I, Br, or F) and the understanding of laser gas kinetics [15].

The energy transfer processes from the Xe(6s) lowest (metastable and resonance) states to molecules were extensively measured by Setser's group [1–3] and in our laboratory [4,7–14], giving in effect a set of rate constants for a number of molecules. If the target molecules were chlorine and/or fluorine donors, XeCl*/XeF* excimers were usually observed among the reaction products [14]. In the case of chlorine donors the formation of XeCl* with photochemical yields from 0.02 for HCl up to 1.0 for Cl₂ was reported [2,5].

Recent years have yielded some data on the quenching rate constants of higher (np) states of rare gases [6,15,16]. They were usually in the range of 10⁻¹¹–10⁻⁹ cm³ s⁻¹. Our pulse radiolysis studies have shown that for molecules such as NH₃, H₂S, H₂O, or freons, the rate constants can even exceed 1 × 10⁻⁹ cm³ s⁻¹ [10,14].

In this paper kinetic data for the energy transfer process and XeCl* excimer formation in the pulse radiolysis of Xe–RCl (RCl = CCl₄ or SOCl₂) systems are presented.

EXPERIMENTAL

Xe–RCl mixtures were irradiated at room temperature (293 ± 2 K) by a 12-ns pulse of 350-keV electrons from a SINUS-5 accelerator in a stainless-steel vacuum-proof chamber of 1000-cm³ volume mounted on the accelerator output (for more details see Refs. 10 and 14).

The purity of the reagents was checked using the GC technique, which allowed us to detect impurities such as N₂, O₂, CH₄, and halogenated compounds with a sensitivity of the order of 10 ppm. The concentration of impurities in Xe never exceeded 10 ppm.

¹ Department of Chemistry, University of Podlasie, 08-110 Siedlce, 3 Maja 54, Poland.

² To whom correspondence should be addressed. e-mail: jowko@ap.siedlce.pl

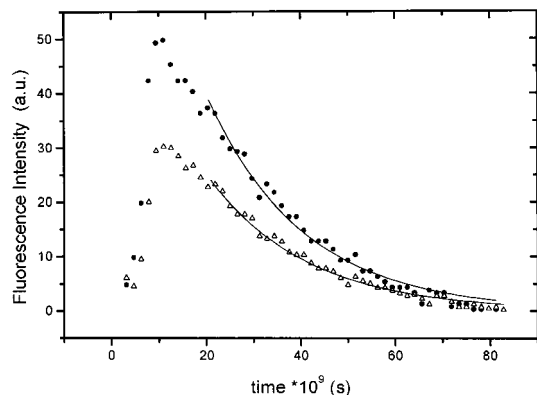


Fig. 1. Time-resolved fluorescence for Xe-SOCl₂ mixtures registered at $\lambda = 240$ nm (●) and 250 nm (△). $P_{\text{Xe}} = 60$ Torr and $P_{\text{SOCl}_2} = 1.0$ Torr. Solid lines, best fit to Eq. (I).

The fluorescence light from the intermediate species formed in the gaseous mixtures after the electron pulse was amplified with an Hamamatsu R928 photomultiplier and, having passed through an Applied Photophysics 7400 0.5-m monochromator, was monitored with a Tektronix 2440 oscilloscope coupled to a PC.

RESULTS AND DISCUSSION

In this experiment the time-resolved fluorescence from Xe-RCl mixtures was recorded at wavelengths $\lambda = 240, 250, 270, 308,$ and 340 nm. The pressure of xenon was kept constant at 60 Torr, while the pressure of RCl varied from 0.2 up to 2.5 Torr. Example data for Xe-SOCl₂ mixture registered at various wavelengths are shown in Figs. 1 and 2. They are typical for all the mixtures investigated.

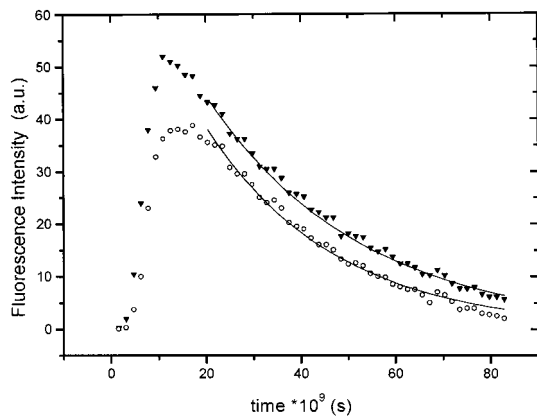


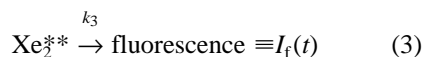
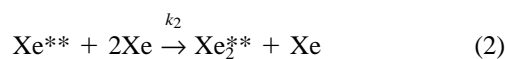
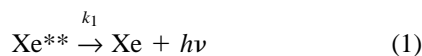
Fig. 2. Time-resolved fluorescence for Xe-SOCl₂ mixtures registered at $\lambda = 308$ nm (▼) and 340 nm (○). $P_{\text{Xe}} = 60$ Torr and $P_{\text{SOCl}_2} = 1.00$ Torr. Solid lines, best fit to Eq. (I).

From earlier studies [16–20] it is known that the irradiation of xenon leads to various manifolds of xenon dimers (Xe_2^*) which fluorize in the range of 149 up to 550 nm if the xenon pressure is close to 1 atm.

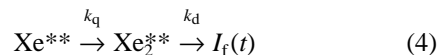
The UV region ($\lambda \geq 220$ nm) of the fluorescence spectrum is characterized by the presence of a continuum with a maximum at 270 nm and is correlated with the transition from higher states of Xe_2^{**} excimers to lower $\text{Xe}_2(O_u^1, 1_u)$ states [16].

It is also known from earlier studies [18,19] that irradiation of Xe with an electron beam populates mainly the Xe(np, nd) excited atoms. In the kinetic model proposed by Eckstrom *et al.* [19], over 50% of all the excited Xe atoms produced by the electron beam were in 6p or higher excited states. In the following they are denoted Xe^{**} .

As demonstrated in previous papers [1,10,14] those states disappear in a consecutive reaction sequence,



which, for simplicity, can be written



The experimentally observed (Figs. 1 and 2) dependences of the fluorescence intensity $I_f(t)$ on time are described by the following double-exponential equation:

$$I_f(t) = [\text{Xe}_2^{**}]_t = \frac{k_q[\text{Xe}^{**}]_0}{(k_d - k_q)} [\exp(-k_q t) - \exp(-k_d t)] \quad (I)$$

where $[\text{Xe}^{**}]_0$ is the initial concentration of atomic excited species, $k_q = k_1 + k_2[\text{Xe}]^2$, and $k_d = k_3$.

In the presence of any molecular admixture (RCl) the quenching reaction (5) should be added to the above reaction scheme:



and K_q is then expressed by Eq. (II):

$$k_q = k_2 + k_3[\text{Xe}]^2 + k_5[\text{RCl}] \quad (II)$$

The simplex algorithm and best-fitting procedure were applied to Eq. (I) to find the unknown k_q parameters, while the k_d values were taken as $k_d = 1.22 \cdot 10^8 \text{ s}^{-1}$ for measurements at $\lambda = 240\text{--}270$ nm [4], $k_d = 3.15 \cdot 10^8 \text{ s}^{-1}$ for measurements at $\lambda = 308$ nm, and $k_d = 1.22 \cdot 10^8$

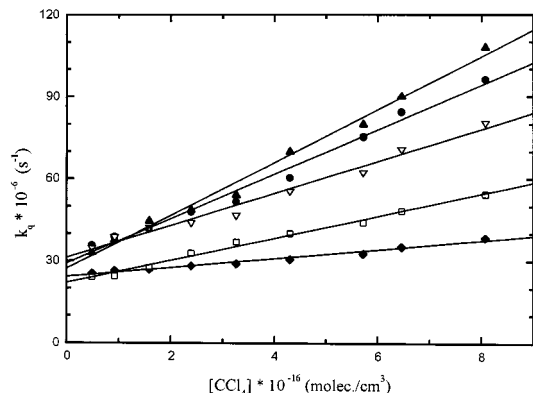


Fig. 3. Plots of k_q versus CCl_4 concentrations [Eq. (III)] for the Xe- CCl_4 system at $\lambda = 240$ nm (▲), 250 nm (●), 270 nm (▽), 308 nm (◆), and 340 nm (□).

cm^{-1} for $\lambda = 340$ nm (see below). Due to the finite electron pulse duration (12 ns) and the Cerenkov effect, the experimental points for $t > 23$ ns were taken for calculations only. Examples of the fittings are shown as the solid lines in Figs. 1 and 2.

As expected, at a constant pressure of xenon, the k_q values obtained were linear functions of the RCl concentrations [Eq. (III)] with linear correlation coefficients $R > 0.98$.

The corresponding plots of $k_q = f[\text{RCl}]$ are shown in Figs. 3 and 4 for Xe- CCl_4 and Xe- SOCl_2 mixtures, respectively.

$$k_q = a + b[\text{RCl}] \quad (\text{III})$$

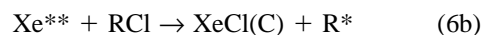
where $a = k_1 + k_2 [\text{Xe}]^2$.

The slope values (b) obtained from those plots are listed in Table I. As shown, the b coefficients diminished with the wavelength. This unexpected wavelength effect

Table I. Slope Values (b) Obtained for Various Wavelengths from Figs. 3 and 4

| RCl | $b * 10^{10} (\text{cm}^3 \text{ s}^{-1})$ | | | | |
|-----------------|--|-----------------------|-----------------------|-----------------------|-----------------------|
| | $\lambda = 240$ nm | $\lambda = 250$ nm | $\lambda = 270$ nm | $\lambda = 308$ nm | $\lambda = 340$ nm |
| CCl_4 | 9.70 | 8.15 | 5.85 | 1.65 | 4.05 |
| SOCl_2 | 14.40 | 13.40 | 5.40 | 2.70 | 5.20 |

on b coefficients seems to be explained only by the recognition that both the molecular admixtures used can produce XeCl^* excimers in the reactions



which (in turn) fluorize in the same wavelength and time regions that Xe_2^{*2} dimers do.

The overlapping effect of the $\text{XeCl}(\text{B,C})$ and Xe_2^{*2} fluorescence spectra is demonstrated in Fig. 5, where the fluorescence intensities registered 30 ns after the electron pulse for Xe- SOCl_2 mixtures are shown together with the control points taken in a similar experiment for pure xenon.

As shown, these intensities are close to each other for $\lambda < 260$ nm. For that reason we supposed that the fluorescence registered in Xe-RCl mixtures at $\lambda < 260$ nm comes mainly from the Xe_2^{*2} excimers, which means, of course, that $k_d = k_3$ and the slope coefficients b . (Table I) are equal to the k_5 rate constants (Table II).

Since the fluorescence intensities of the Xe-RCl mixtures at $\lambda > 270$ nm were several times higher than those observed in pure xenon (Fig. 5), we have assumed that the contribution of reaction (3) to the overall fluores-

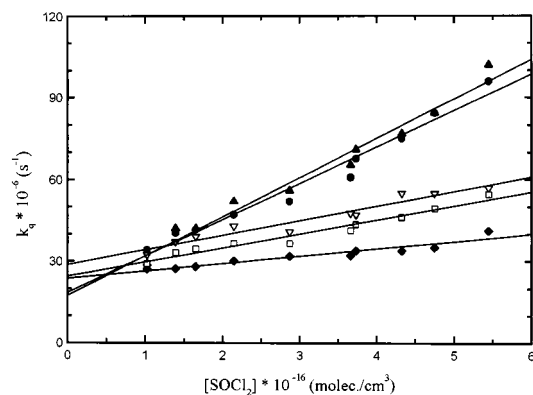


Fig. 4. Plots of k_q on SOCl_2 concentrations [Eq. (III)] for the Xe- SOCl_2 system at $\lambda = 240$ nm (▲), 250 nm (●), 270 nm (▽), 308 nm (◆), and 340 nm (□).

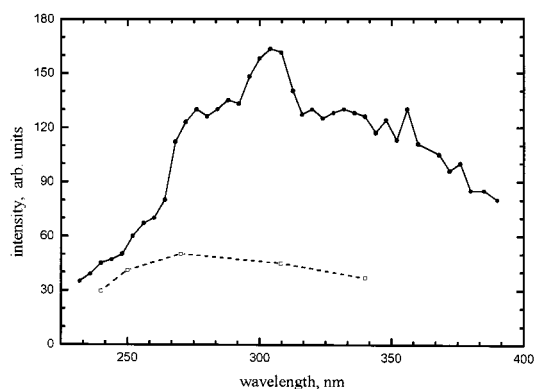


Fig. 5. Fluorescence spectrum of a Xe- SOCl_2 mixture (●); control point taken in the same experiment for pure Xe (□). $P_{\text{Xe}} = 60$ Torr; $P_{\text{SOCl}_2} = 1.0$ Torr. Spectra were registered 30 ns after the electron pulse.

Table II. Rate Constants and Efficiencies (Γ) of XeCl* Excimer Formation

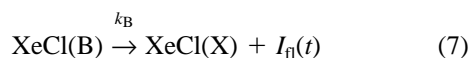
| RCl | $k_5 * 10^{10}$ (cm ³ s ⁻¹) | $k_{6b} * 10^{10}$ (cm ³ s ⁻¹) | $k_{6c} * 10^{10}$ (cm ³ s ⁻¹) | $\Gamma_{\text{XeCl(B)}}$ | $\Gamma_{\text{XeCl(C)}}$ | $\Gamma_{\text{XeCl(B,C)}}$ | k_{6c}/k_{6b} |
|-------------------|---|--|--|---------------------------|---------------------------|-----------------------------|------------------------------|
| CCl ₄ | 9.7 ± 0.3 (6.3, ^a 6.0 ^b) | 1.65 ± 0.15 (0.9 ^a) | 4.05 ± 0.20 (0.6 ^a) | 0.17 ± 0.01 (0.143) | 0.42 ± 0.01 (0.095) | 0.59 ± 0.02 (0.24) | 2.45 (0.67 ^a) |
| SOCl ₂ | 14.4 ± 0.5 (4.0, ^a 5.8 ^b) | 2.7 ± 0.15 (1.2 ^b) | 5.20 ± 0.15 (0.8 ^b) | 0.19 ± 0.01 (0.21) | 0.36 ± 0.01 0.14 | 0.55 ± 0.02 0.34 | 1.93 (0.67 ^a) |

^a Data for Xe(³P₂) states from Ref. 2.

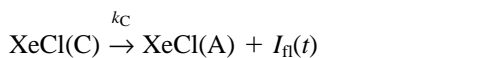
^b Data for Xe(³p₁) states from Ref. 8.

cence is negligible and supposed for further considerations that the fluorescence registered at 308 and 340 nm comes only from Xe(B,C) states.

From previous comprehensive and more refined studies [20–24] it is well known that the emission at 308 nm should be assigned to B–X transitions,



and those observed at 340 nm to C–A transitions,

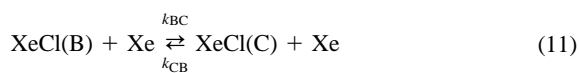
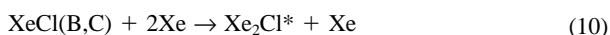


$$k_B = 9.1 \times 10^7 \text{ s}^{-1}; \quad (8)$$

$$k_C = 8.3 \times 10^6 \text{ s}^{-1} \quad [15]$$

Therefore, the slope coefficients b , listed in Table I, at $\lambda = 308$ and 340 nm are equal to k_{6a} and k_{6b} , respectively.

Of course, reactions (7) and (8) are not the only decay channels of the XeCl(B,C) excimers and processes (9)–(11) should have been included in the reaction sequence considered for calculations.



$$k_9 = 5 \times 10^{-12} \text{ cm}^3 \text{ s}^{-1};$$

$$k_{10} = (1 - 0.8) \times 10^{-30} \text{ cm}^6 \text{ s}^{-1} \quad [24]$$

$$k_{\text{BC}} = 1.1 \times 10^{-10} \text{ cm}^3 \text{ s}^{-1};$$

$$k_{\text{CB}} = 0.74 \times 10^{-10} \text{ cm}^3 \text{ s}^{-1} \quad [15]$$

Having that, we obtained the expressions [Eqs. (IV) and (V)] which allowed us to find the k_d values being taken for calculations in Eq. (I):

$$k_d^{\text{XeCl(B)}} = k_B + k_9 [\text{Xe}] + k_{\text{BC}} [\text{Xe}] \quad (IV)$$

$$+ k_{10} [\text{Xe}]^2 = 3.15 \times 10^8 \text{ s}^{-1}$$

$$k_d^{\text{XeCl(C)}} = k_C + k_9 [\text{Xe}] + k_{\text{CB}} [\text{Xe}] \quad (V)$$

$$+ k_{10} [\text{Xe}]^2 = 1.22 \times 10^8 \text{ s}^{-1}$$

All kinetics data found in these investigations are listed in Table II. As shown, the quenching rate constants (k_5) are much higher than those found for Xe(6s) states [2,8]. The same effect, i.e., a more than twofold increase in the rate constants was reported by Setser *et al.* [25] for Xe(6p)–Cl₂ interactions as well as by Wojciechowski *et al.* [10,13] in studies on Xe–CH₄ and Xe–CH₂F₂ systems [10,13], where the k_5 rate constants found for Xe(6p,6d) manifolds were a few times higher from those obtained for Xe(6s) states.

At the same time the efficiency (Γ_{XeCl^*}) of the formation of XeCl* excimers is also significantly higher compared to that for Xe(6s) states. The corresponding Γ values increase from 0.24 to 0.59 and from 0.34 to 0.55 for CCl₄ and SOCl₂, respectively. The same tendency was also observed by Ku and Setser [25] for Xe(6p,d) manifolds in Xe–HCl or CCl₄ systems, where Γ_{XeCl} was equal to 0.8 and 0.7, respectively, compared to 0.02 and 0.24 for Xe(6s) states [10].

Also, the formation of XeCl(C) states in pulse radiolysis seems to be preferred, and the rate ratios of k_{6c}/k_{6b} increase from 0.67 to 1.97 and 2.45 for CCl₄ and SOCl₂, respectively (Table II). The rate of production of XeCl(C) excimers from Xe(6p,6d) states is over six times faster than that from Xe(6s) states, while the rate of production of XeCl(B) states increases only two times. The contribution ($\Gamma_{\text{XeCl(B)}}$) of XeCl(B) states to the overall (Γ_{XeCl^*}) XeCl(B,C) excimers yields remain on the same level, however, for both Xe(6p,6d) and Xe(6s) states.

SUMMARY

(1) The rate constants (k_5) of the energy transfer from highly excited Xe** atoms produced under pulse radiolysis conditions were found for the first time for

CCl₄ and SOCl₂ molecules. The values are close to those obtained under the same conditions in Refs. 8 and 9 for other molecules.

(2) The efficiency and the rate constants (k_{6a} and k_{6b}) of the formation of XeCl(B) and XeCl(C) excimers were also found.

(3) The Xe(6p,d) manifolds predominant in pulse radiolysis must be responsible for the enhanced yield of XeCl(C) states ($\Gamma_{\text{XeCl(C)}}$) compared to that observed for Xe(6s) manifolds [2, 8], while the yield of XeCl(B) seems to be the same.

REFERENCES

1. R. Cooper, R. Denison, P. Zeglinski, C. R. Roy, and H. Gillis (1983) *J. Appl. Phys.* **54**, 3053.
2. J. E. Velazco, J. H. Klots, and D. W. Setser (1978) *J. Chem. Phys.* **69**, 1978.
3. Xiaoshan Chen and D. W. Setser (1991) *J. Phys. Chem.* **95**, 8473.
4. A. Birot, H. Brunet, J. Galy, P. Milletand, and J. L. Teysier (1975) *J. Chem. Phys.* **63**, 1469.
5. J. K. Ku and D. W. Setser (1986) *J. Chem. Phys.* **84**, 4304.
6. M. R. Bruce, W. B. Layne, E. Meyer, and J. W. Keto (1990) *J. Chem. Phys.* **92**, 420.
7. A. Jowko, E. Bartkiewicz, and M. Forys (1990) *J. Radioanal. Nucl. Chem. Lett.* **140**, 21.
8. K. Wojciechowski, M. Rosa, A. Jówko, and M. Forys (1993) *Nukleonika* **38**, 31.
9. K. Wojciechowski, M. Rosa, M. Symanowicz, A. Jówko, and Forys (1994) *Nukleonika* **39**, 35.
10. A. Jówko, J. Kowalczyk, K. Wojciechowski, and M. Forys (1996) *Radiat. Phys. Chem.* **48**, 481.
11. K. Wojciechowski (1998) *Radiat. Phys. Chem.* **51**, 159.
12. K. Wojciechowski (1998) *Radiat. Phys. Chem.* **53**, 37–46.
13. K. Wojciechowski (1998) *Radiat. Phys. Chem.* **53**, 47–53.
14. K. Wojciechowski, J. Kowalczyk, and A. Jówko (1998) *Radiat. Phys. Chem.* **53**, 417–424.
15. G. Inoue, J. K. Ku, and D. W. Setser (1984) *J. Chem. Phys.* **80**, 6006.
16. G. Inoue, J. K. Ku, and D. W. Setser (1984) *J. Chem. Phys.* **81**, 5760.
17. P. Millet, A. Birot, J. Galy, B. Pons-Germain, and J. L. Teysier (1978) *J. Chem. Phys.* **69**, 92.
18. O. Dutuit, M. C. Castex, J. Le Calve, and M. Lavolle (1980) *J. Chem. Phys.* **73**, 3107.
19. D. J. Eckstrom, H. H. Nakano, D. C. Lorents, T. Rothen, J. A. Betts, M. E. Lainhart, D. A. Dakin, and J. E. Maenchen (1988) *J. Appl. Phys.* **64**, 1679.
20. T. H. Johnson, H. E. Cartland, T. C. Genoni, and A. M. Hunter (1989) *J. Appl. Phys.* **66**, 5707.
21. H. C. Brashears and D. W. Setser (1980) *J. Phys. Chem.* **84**, 224.
22. H. C. Brashears and D. W. Setser, (1980) *J. Phys. Chem.* **84**, 2495.
23. T. O. Nelson and D. W. Setser, (1993) *J. Phys. Chem.* **97**, 2585.
24. E. Quinones, Y. C. Yu, D. W. Setser, and G. Lo (1990) *J. Chem. Phys.* **93**, 333.
25. J. K. Ku and D. W. Setser (1986) *Appl. Phys. Lett.* **48**, 687.